Supplement of Earth Syst. Dynam., 16, 1671–1698, 2025
https://doi.org/10.5194/esd-16-1671-2025-supplement

Earth System Dynamics
Open Access
EGU

Supplement of

Sensitivity of winter Arctic amplification in NorESM2

Lise Seland Graff et al.

Correspondence to: Lise Seland Graff (lise.s.graff@met.no)

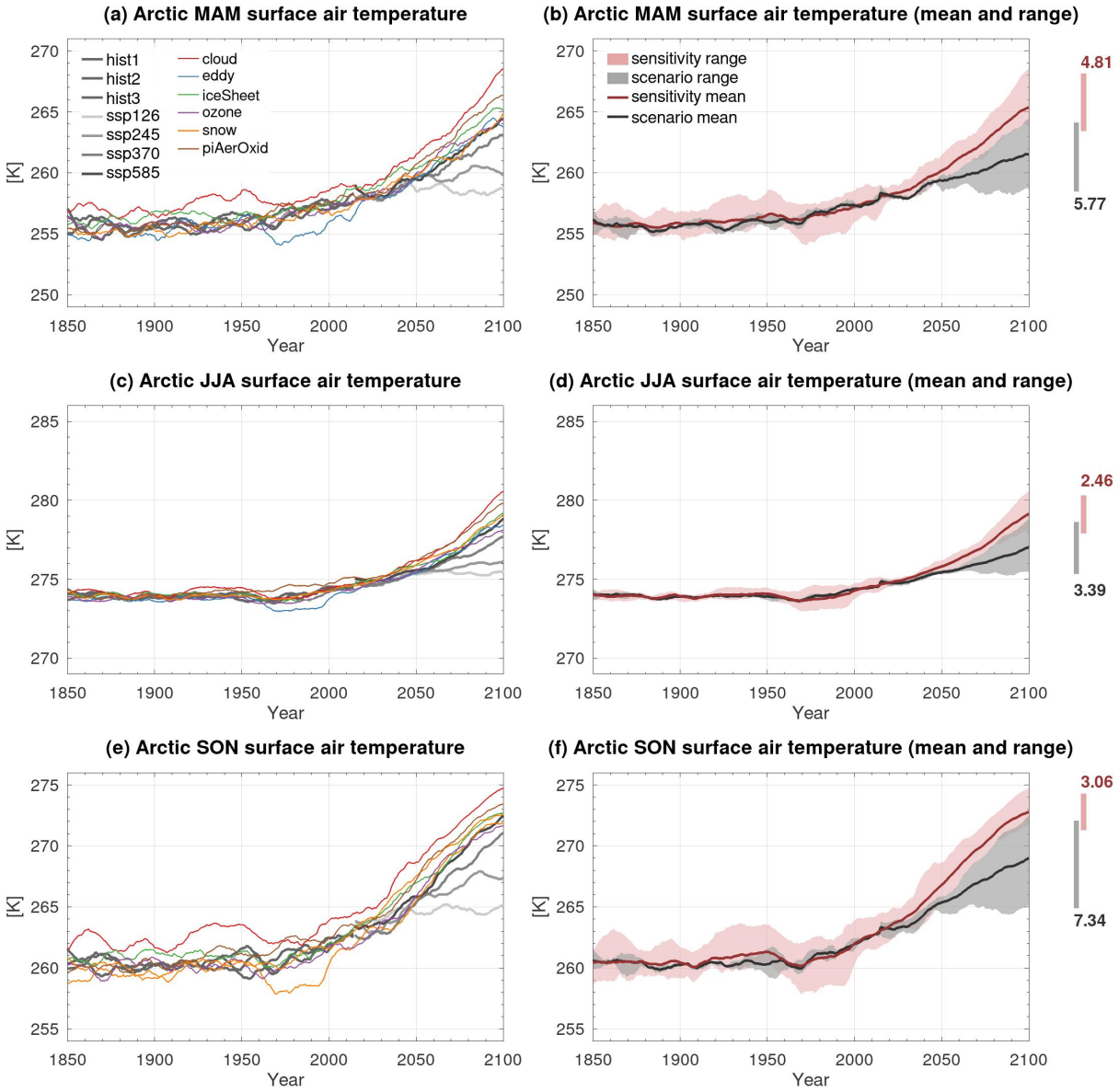

Figure S1. Time evolution of spring (March–May; MAM; a–b), summer (June–August; JJA; c–d), and fall (September–November; SON; e–f) Arctic surface temperature for 1850–2100. In a, c, and e, the individual lines show the CMIP6 historical realizations (hist1, hist2, and hist3), four future scenarios (ssp126, ssp245, ssp370, ssp585), and the six sensitivity experiments (*cloud*, *eddy*, *iceSheet*, *ozone*, *snow*, and *piAerOxid*) (see legend in a). In b, d, and f, the lines show the mean warming for the scenarios (grey) and sensitivity experiments (red) and the shading shows the warming range between the experiments with strongest and weakest warming (see legend in b). To highlight the end-of-the-century warming range, the difference between the experiment with strongest and weakest warming in 2100 is additionally shown in terms of the numbers and vertical bars to the right of b, d, and f. A 10-year running mean has been applied. Units are in K.

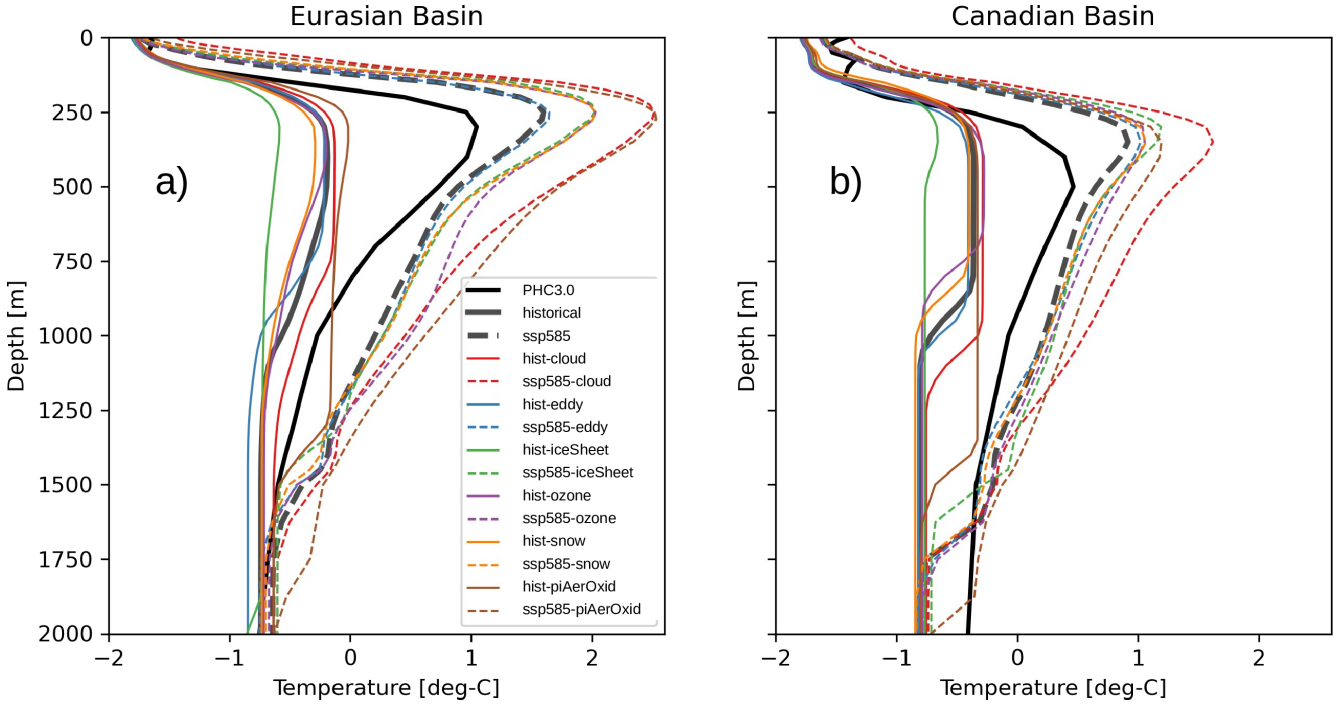

Figure S2. Historical (solid lines) and future (dashed lines) vertical ocean temperature profiles averaged for the Eurasian (a) and Canadian Basins (b). Both panels show the historical and ssp585-based experiments for the baseline (historical and ssp585; grey lines), *cloud* (hist-cloud and ssp585-cloud; red lines), *eddy* (hist-eddy and ssp585-eddy; blue lines), *iceSheet* (hist-iceSheet and ssp585-icesheet; green lines), *ozone* (hist-ozone and ssp585-ozone; purple lines), *snow* (hist-snow and ssp585-snow; orange lines), and *piAerOxid* (hist-piAerOxid and ssp585-piAerOxid; brown lines) experiments. Observations (black solid lines) are from the Polar Science Center Hydrographic Climatology (PHC Steele et al., 2001) version 3.0. Units are in °C.

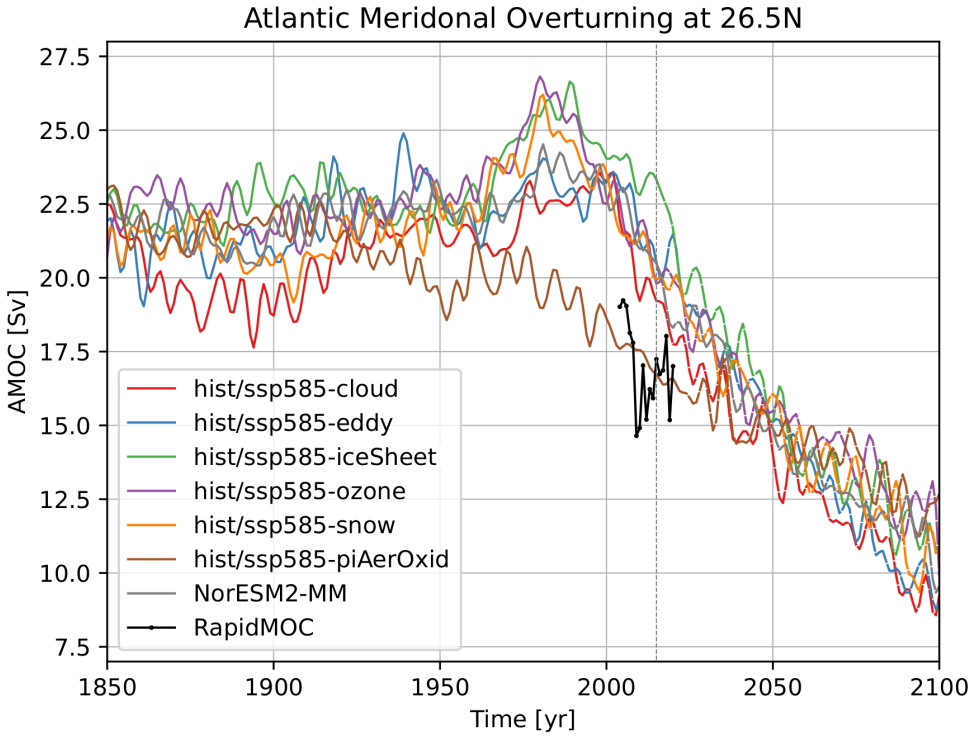

Figure S3. Time evolution of the Atlantic meridional overturning circulation at 26.5°N for the baseline (historical and ssp585; grey line) *cloud* (hist-cloud and ssp585-cloud; red line), *eddy* (hist-eddy and ssp585-eddy; blue line), *iceSheet* (hist-iceSheet and ssp585-iceSheet; green line), *ozone* (hist-ozone and ssp585-ozone; purple line), *snow* (hist-snow and ssp585-snow; orange line), and *piAerOxid* (hist-piAerOxid and ssp585-piAerOxid; brown line) experiments. Also shown is the RapidMOC estimate (black line; McCarthy et al., 2015). Units are in Sv.

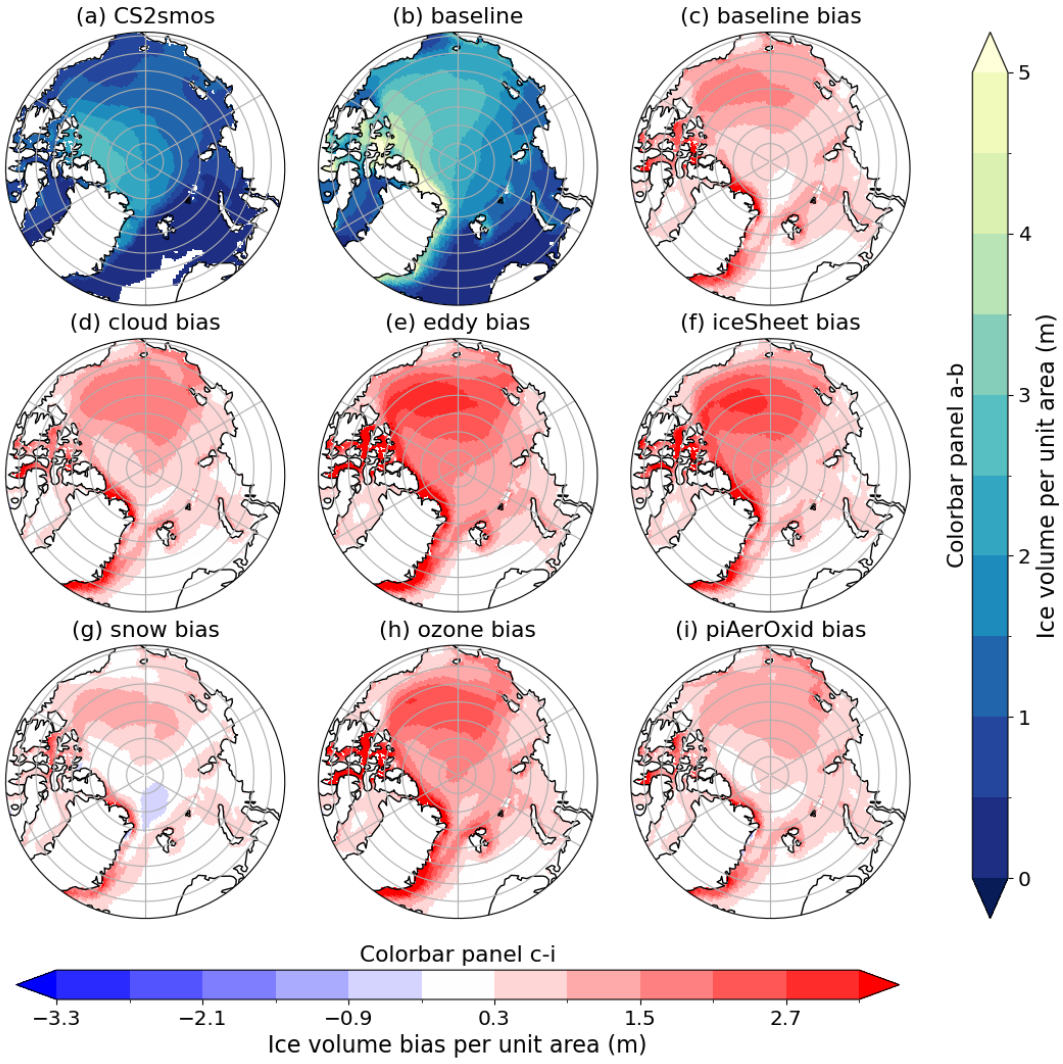

Figure S4. Spatial distribution of observed winter (December–February; DJF) sea-ice volume from CryoSat-2 – SMOS for the period 2011–2022 (a), and for the baseline experiment (b). Bias in sea-ice volume with respect to the observations for the historical baseline (c), *cloud* (d), *eddy* (e), *iceSheet* (f), *snow* (g), *ozone* (h), and *piAerOxid* experiments (i). The model climatologies are based on years 2011–2014 from the historical experiments and years 2015–2022 from the ssp585 experiments. Units are in volume per unit area (m).

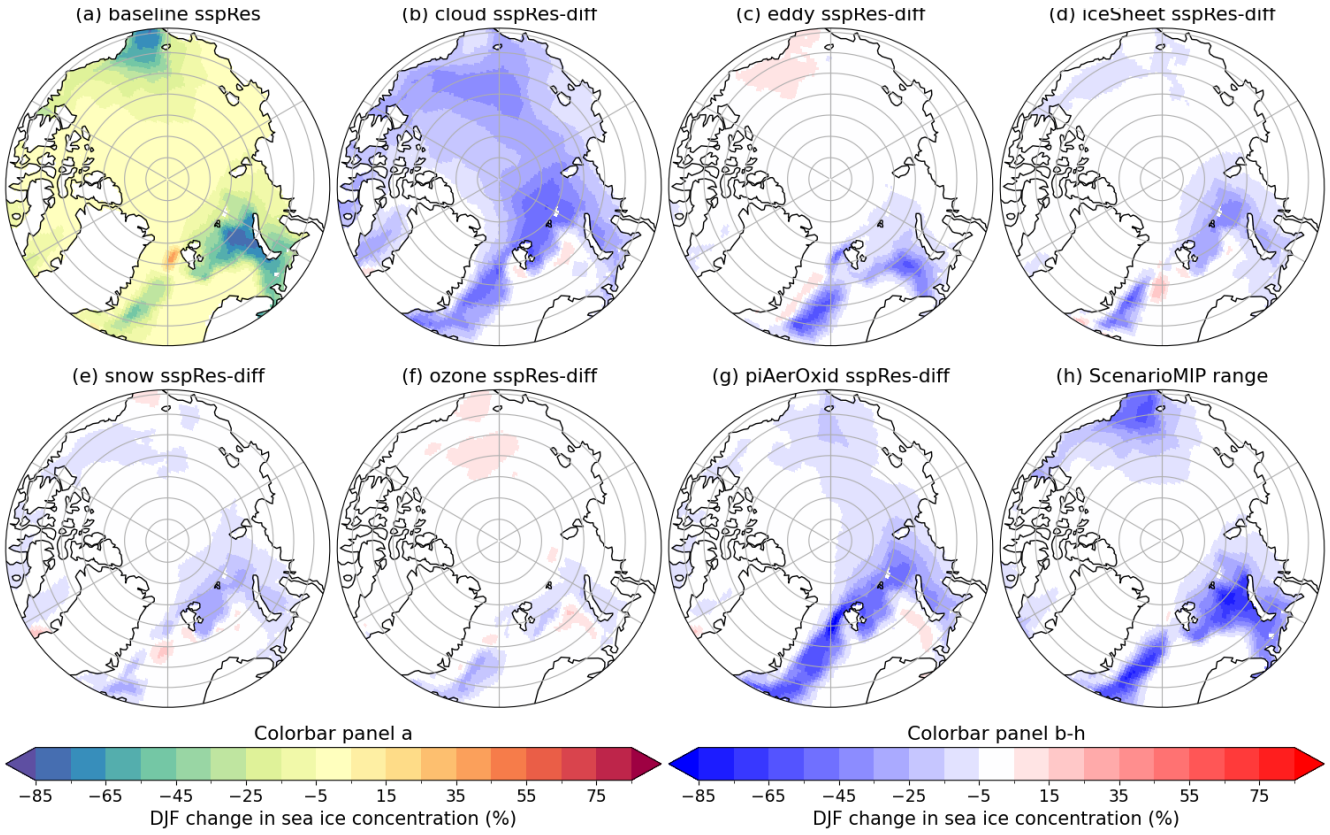

Figure S5. Spatial distribution of the future changes in sea-ice concentration during winter for the future response (sspRes; Table 2 in the main text) for the baseline experiments (a) and the future response difference (sspRes-diff; Table 2 in the main text) for *cloud* (b), *eddy* (c), *iceSheet* (d), *snow* (e), *ozone* (f), and *piAerOxid* (g), and the ScenarioMIP range (ssp585−ssp126; h). Units are in % of surface area.

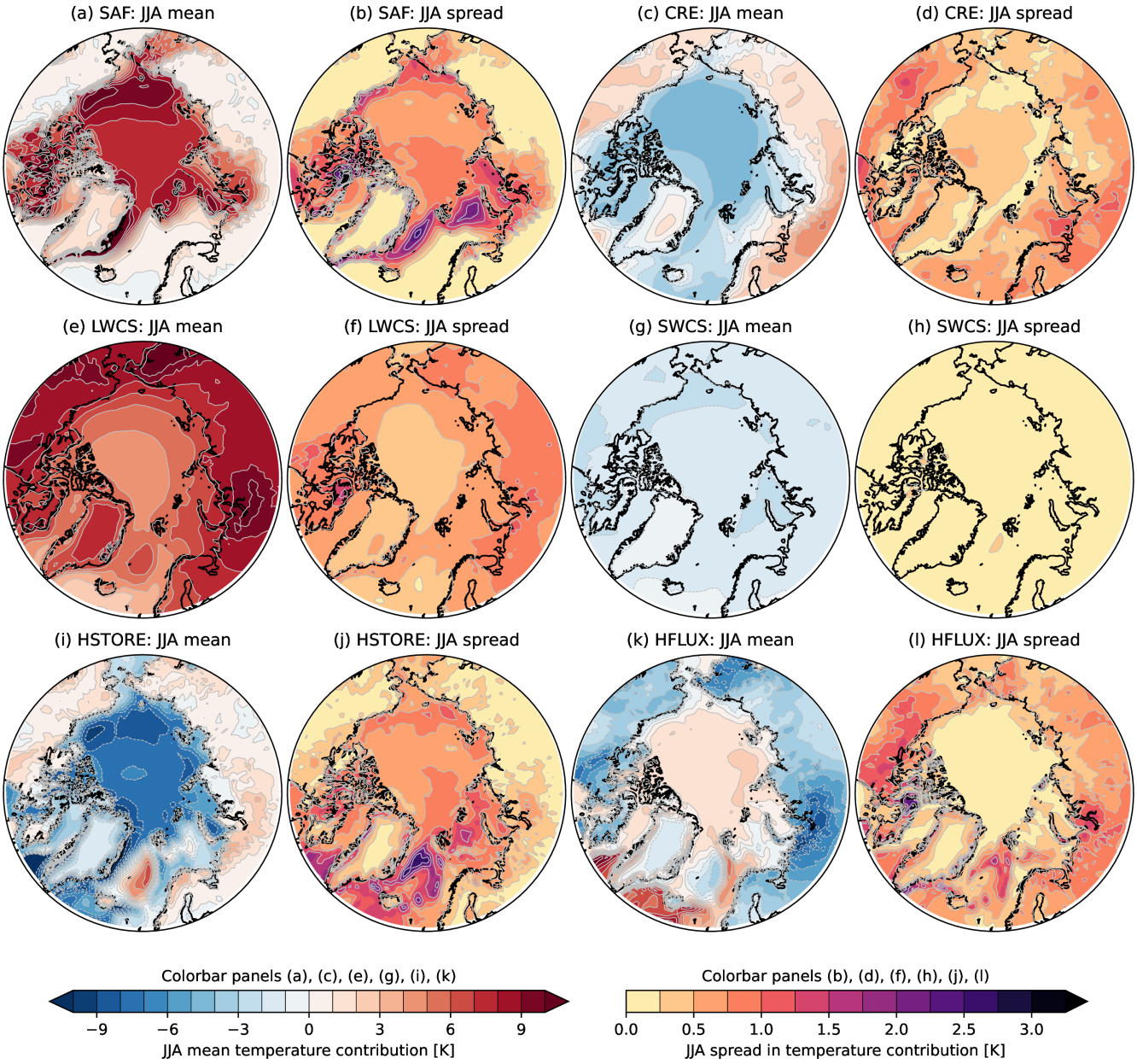

Figure S6. Spatial distribution of summer (JJA) ensemble-mean (a, c, e, g, i, k) and spread (b, d, f, h, j, l), computed across the CMIP6 baseline and the NEEMS experiments (*cloud*, *eddy*, *iceSheet*, *snow*, and *ozone*), for the future response (Table 2 in the main text) in the surface temperature decomposition terms: SAF (a–b), CRE (c–d), LWCS (e–f), SWCF (g–h), HSTORE (i–j), and HFLUX (k–l). Units are in K.

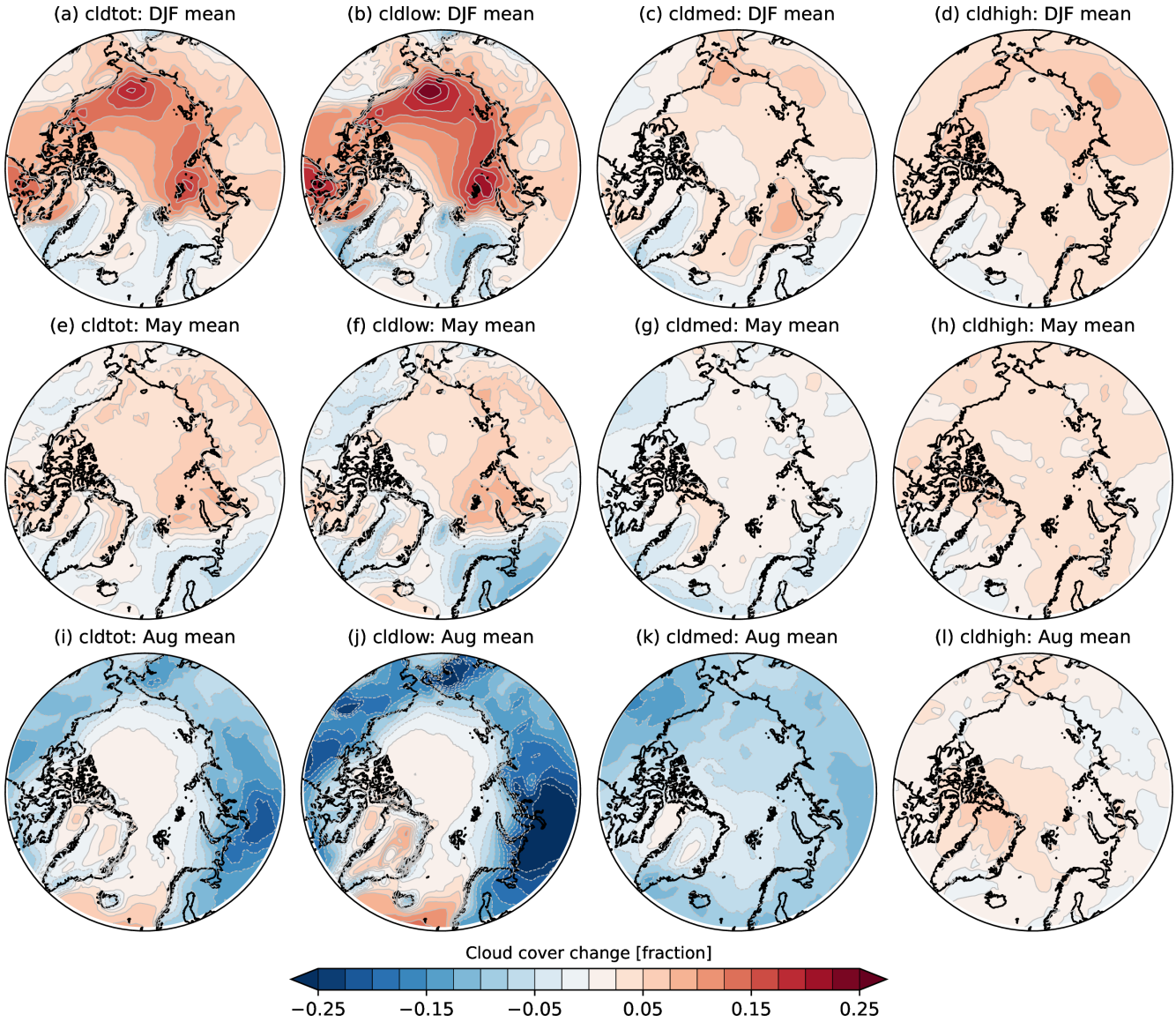

Figure S7. Spatial distribution of the ensemble mean, computed across the baseline and the NEEMS experiments (*cloud*, *eddy*, *iceSheet*, *snow*, and *ozone*), for the future response (Table 2 in the main text) for total cloud cover (a, e, i), low-level cloud cover (b, f, j), medium-level cloud cover (c, g, k), and high-level cloud cover (d, h, l) for winter (DJF; a–d), May (e–h), and August (i–l). Units are in fraction.

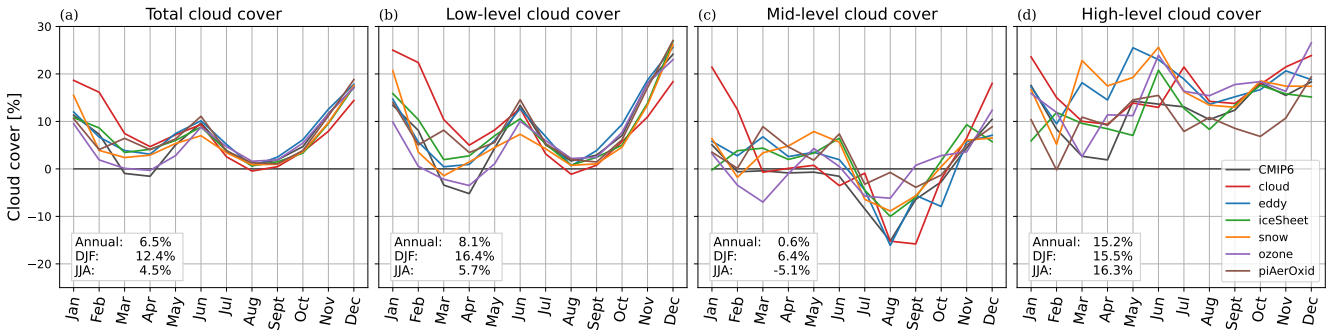

Figure S8. Monthly evolution of the future response (Table 2 in the main text) in total cloud cover (a), low-level cloud cover (b), medium-level cloud cover (c), and high-level cloud cover (d) for the Arctic Ocean (defined as 80°N–90°N) for the CMIP6 baseline (black line), *cloud* (red line), *eddy* (blue line), *iceSheet* (green line), *snow* (orange line), *ozone* (purple line), and *piAerOxid* (brown line). The annual, DJF, and JJA mean values, averaged across the baseline and five NEEMS experiments (*cloud*, *eddy*, *iceSheet*, *snow*, and *ozone*), are shown in the right legend. Units are in percentage change.

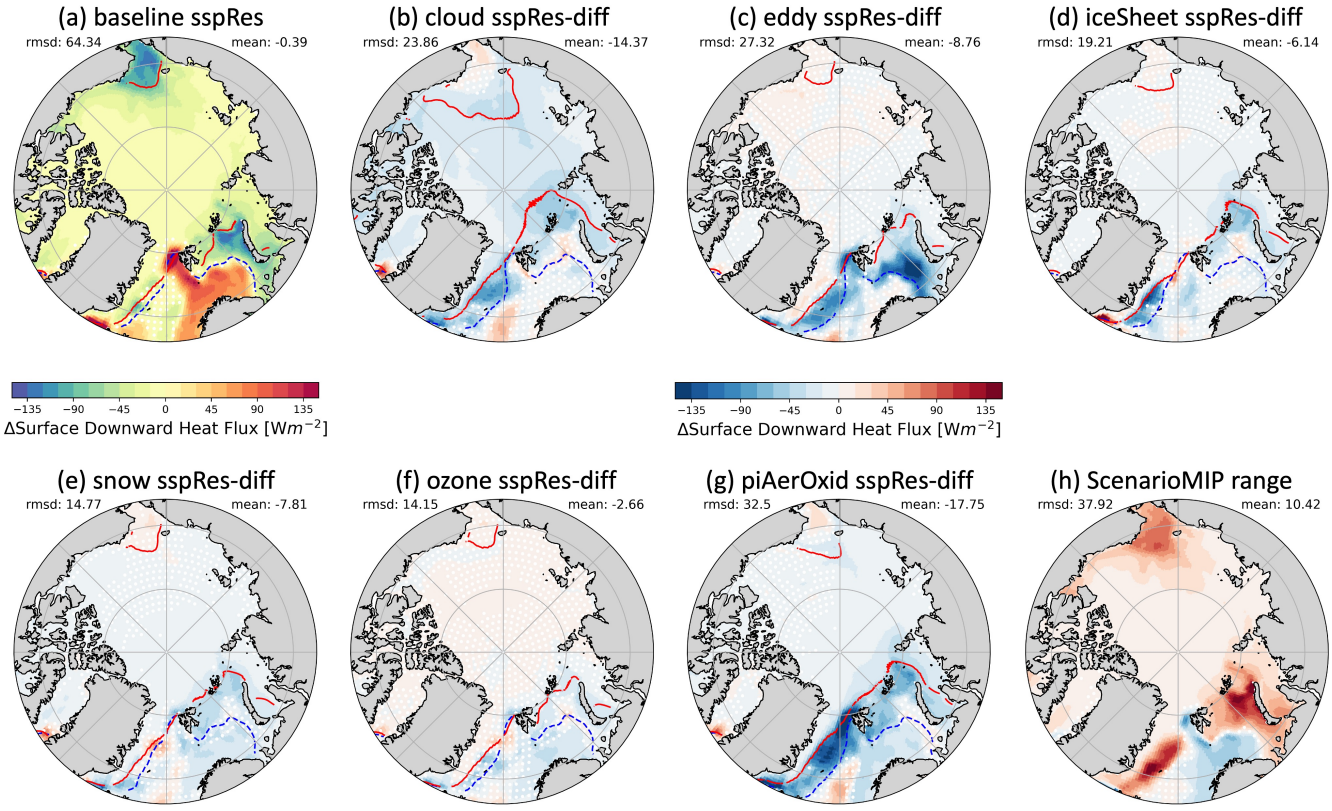

Figure S9. Spatial distribution of future changes in Arctic ocean heat flux (colors) during winter (DJF) for the future response (sspRes; Table 2 in the main text) for the baseline experiments (a) and the future response difference (sspRes-diff; Table 2 in the main text) for *cloud* (b), *eddy* (c), *iceSheet* (d), *snow* (e), *ozone* (f), and *piAerOxid* (g), and the ScenarioMIP range (ssp585−ssp126; h). The dashed-blue and solid-red lines depict the 50% sea-ice extent averaged over the contemporary period (1985–2015) and end of the 21st century (2071–2100). The area average (mean) and the root-mean-square-difference (rmsd) of the field shown (colors) is given in the upper right and left corners of each panel. White dots indicate non-significant changes according to a two-sided T-test. Note that we use different color scales and contour levels for a (left color bar) and b–h (right color bar). Units are in W m^{-2}.

Table S1. List of CMIP6 models used in Fig. 17 in the main text and the associated references.

Model name	**Reference**
ACCESS-CM2	Law et al. (2017)
ACCESS-ESM1-5	Law et al. (2017)
CAMS-CSM1-0	Rong et al. (2019)
CanESM5	Swart et al. (2019)
CanESM5-CanOE	Swart et al. (2019)
CESM2-WACCM	Liu et al. (2019)
CNRM-CM6-1	Séférian et al. (2019)
CNRM-CM6-1-HR	Séférian et al. (2019)
CNRM-ESM2-1	Séférian et al. (2019)
GFDL-CM4	Held et al. (2019)
GFDL-ESM4	Dunne et al. (2020)
IPSL-CM6A-LR	Boucher et al. (2020)
MIROC-ES2L	Hajima et al. (2020)
MPI-ESM1-2-HR	Müller et al. (2018)
MPI-ESM1-2-LR	Mauritsen et al. (2019)
MRI-ESM2-0	Yukimoto et al. (2019)
NorESM2-LM	Seland et al. (2020)
NorESM2-MM	Seland et al. (2020)
UKESM1-0-LL	Sellar et al. (2019)

References

Boucher, O., Servonnat, J., Albright, A. L., Aumont, O., Balkanski, Y., Bastrikov, V., Bekki, S., Bonnet, R., Bony, S., Bopp, L., Braconnot, P., Brockmann, P., Cadule, P., Caubel, A., Cheruy, F., Codron, F., Cozic, A., Cugnet, D., D'Andrea, F., Davini, P., de Lavergne, C., Denvil, S., Deshayes, J., Devilliers, M., Ducharne, A., Dufresne, J.-L., Dupont, E., Éthé, C., Fairhead, L., Falletti, L., Flavoni, S., Foujols, M.-A., Gardoll, S., Gastineau, G., Ghattas, J., Grandpeix, J.-Y., Guenet, B., Guez, Lionel, E., Guilyardi, E., Guimberteau, M., Hauglustaine, D., Hourdin, F., Idelkadi, A., Joussaume, S., Kageyama, M., Khodri, M., Krinner, G., Lebas, N., Levavasseur, G., Lévy, C., Li, L., Lott, F., Lurton, T., Luyssaert, S., Madec, G., Madeleine, J.-B., Maignan, F., Marchand, M., Marti, O., Mellul, L., Meurdesoif, Y., Mignot, J., Musat, I., Ottlé, C., Peylin, P., Planton, Y., Polcher, J., Rio, C., Rochetin, N., Rousset, C., Sepulchre, P., Sima, A., Swingedouw, D., Thiéblemont, R., Traore, A. K., Vancoppenolle, M., Vial, J., Vialard, J., Viovy, N., and Vuichard, N.: Presentation and Evaluation of the IPSL-CM6A-LR Climate Model, Journal of Advances in Modeling Earth Systems, 12, e2019MS002 010, https://doi.org/https://doi.org/10.1029/2019MS002010, e2019MS002010 10.1029/2019MS002010, 2020.

Dunne, J. P., Horowitz, L. W., Adcroft, A. J., Ginoux, P., Held, I. M., John, J. G., Krasting, J. P., Malyshev, S., Naik, V., Paulot, F., Shevliakova, E., Stock, C. A., Zadeh, N., Balaji, V., Blanton, C., Dunne, K. A., Dupuis, C., Durachta, J., Dussin, R., Gauthier, P. P. G., Griffies, S. M., Guo, H., Hallberg, R. W., Harrison, M., He, J., Hurlin, W., McHugh, C., Menzel, R., Milly, P. C. D., Nikonov, S., Paynter, D. J., Ploshay, J., Radhakrishnan, A., Rand, K., Reichl, B. G., Robinson, T., Schwarzkopf, D. M., Sentman, L. T., Underwood, S., Vahlenkamp, H., Winton, M., Wittenberg, A. T., Wyman, B., Zeng, Y., and Zhao, M.: The GFDL Earth System Model Version 4.1 (GFDL-ESM 4.1): Overall Coupled Model Description and Simulation Characteristics, Journal of Advances in Modeling Earth Systems, 12, e2019MS002 015, https://doi.org/https://doi.org/10.1029/2019MS002015, e2019MS002015 2019MS002015, 2020.

Hajima, T., Watanabe, M., Yamamoto, A., Tatebe, H., Noguchi, M. A., Abe, M., Ohgaito, R., Ito, A., Yamazaki, D., Okajima, H., Ito, A., Takata, K., Ogochi, K., Watanabe, S., and Kawamiya, M.: Development of the MIROC-ES2L Earth system model and the evaluation of biogeochemical processes and feedbacks, Geoscientific Model Development, 13, 2197–2244, https://doi.org/10.5194/gmd-13-2197-2020, 2020.

Held, I. M., Guo, H., Adcroft, A., Dunne, J. P., Horowitz, L. W., Krasting, J., Shevliakova, E., Winton, M., Zhao, M., Bushuk, M., Wittenberg, A. T., Wyman, B., Xiang, B., Zhang, R., Anderson, W., Balaji, V., Donner, L., Dunne, K., Durachta, J., Gauthier, P. P. G., Ginoux, P., Golaz, J.-C., Griffies, S. M., Hallberg, R., Harris, L., Harrison, M., Hurlin, W., John, J., Lin, P., Lin, S.-J., Malyshev, S., Menzel, R., Milly, P. C. D., Ming, Y., Naik, V., Paynter, D., Paulot, F., Ramaswamy, V., Reichl, B., Robinson, T., Rosati, A., Seman, C., Silvers, L. G., Underwood, S., and Zadeh, N.: Structure and Performance of GFDL's CM4.0 Climate Model, Journal of Advances in Modeling Earth Systems, 11, 3691–3727, https://doi.org/https://doi.org/10.1029/2019MS001829, 2019.

Law, R. M., Ziehn, T., Matear, R. J., Lenton, A., Chamberlain, M. A., Stevens, L. E., Wang, Y.-P., Srbinovsky, J., Bi, D., Yan, H., and Vohralik, P. F.: The carbon cycle in the Australian Community Climate and Earth System Simulator (ACCESS-ESM1) – Part 1: Model description and pre-industrial simulation, Geoscientific Model Development, 10, 2567–2590, https://doi.org/10.5194/gmd-10-2567-2017, 2017.

Liu, S.-M., Chen, Y.-H., Rao, J., Cao, C., Li, S.-Y., Ma, M.-H., and Wang, Y.-B.: Parallel Comparison of Major Sudden Stratospheric Warming Events in CESM1-WACCM and CESM2-WACCM, Atmosphere, 10, https://doi.org/10.3390/atmos10110679, 2019.

Mauritsen, T., Bader, J., Becker, T., Behrens, J., Bittner, M., Brokopf, R., Brovkin, V., Claussen, M., Crueger, T., Esch, M., Fast, I., Fiedler, S., Fläschner, D., Gayler, V., Giorgetta, M., Goll, D. S., Haak, H., Hagemann, S., Hedemann, C., Hohenegger, C., Ilyina, T., Jahns, T., Jimenéz-de-la Cuesta, D., Jungclaus, J., Kleinen, T., Kloster, S., Kracher, D., Kinne, S., Kleberg, D., Lasslop, G., Kornblueh, L.,

Marotzke, J., Matei, D., Meraner, K., Mikolajewicz, U., Modali, K., Möbis, B., Müller, W. A., Nabel, J. E. M. S., Nam, C. C. W., Notz, D., Nyawira, S.-S., Paulsen, H., Peters, K., Pincus, R., Pohlmann, H., Pongratz, J., Popp, M., Raddatz, T. J., Rast, S., Redler, R., Reick, C. H., Rohrschneider, T., Schemann, V., Schmidt, H., Schnur, R., Schulzweida, U., Six, K. D., Stein, L., Stemmler, I., Stevens, B., von Storch, J.-S., Tian, F., Voigt, A., Vrese, P., Wieners, K.-H., Wilkenskjeld, S., Winkler, A., and Roeckner, E.: Developments in the MPI-M Earth System Model version 1.2 (MPI-ESM1.2) and Its Response to Increasing CO2, Journal of Advances in Modeling Earth Systems, 11, 998–1038, https://doi.org/https://doi.org/10.1029/2018MS001400, 2019.

McCarthy, G. D., Smeed, D. A., Johns, W. E., Frajka-Williams, E., Moat, B. I., Rayner, D., Baringer, M. O., Meinen, C. S., Collins, J., and Bryden, H. L.: Measuring the Atlantic Meridional Overturning Circulation at 26°N, Progress in Oceanography, 130, 91–111, https://doi.org/10.1016/j.pocean.2014.10.006, 2015.

Müller, W. A., Jungclaus, J. H., Mauritsen, T., Baehr, J., Bittner, M., Budich, R., Bunzel, F., Esch, M., Ghosh, R., Haak, H., Ilyina, T., Kleine, T., Kornblueh, L., Li, H., Modali, K., Notz, D., Pohlmann, H., Roeckner, E., Stemmler, I., Tian, F., and Marotzke, J.: A Higher-resolution Version of the Max Planck Institute Earth System Model (MPI-ESM1.2-HR), Journal of Advances in Modeling Earth Systems, 10, 1383–1413, https://doi.org/https://doi.org/10.1029/2017MS001217, 2018.

Rong, X., Li, J., Chen, H., Xin, Y., Su, J., Hua, L., Zhou, T., Qi, Y., Zhang, Z., Zhang, G., and Li, J.: The CAMS Climate System Model and a Basic Evaluation of Its Climatology and Climate Variability Simulation, Journal of Meteorological Research, 32, https://doi.org/10.1007/s13351-018-8058-x, 2019.

Seland, Ø., Bentsen, M., Olivié, D., Toniazzo, T., Gjermundsen, A., Graff, L. S., Debernard, J. B., Gupta, A. K., He, Y.-C., Kirkevåg, A., Schwinger, J., Tjiputra, J., Aas, K. S., Bethke, I., Fan, Y., Griesfeller, J., Grini, A., Guo, C., Ilicak, M., Karset, I. H. H., Landgren, O., Liakka, J., Moseid, K. O., Nummelin, A., Spensberger, C., Tang, H., Zhang, Z., Heinze, C., Iversen, T., and Schulz, M.: Overview of the Norwegian Earth System Model (NorESM2) and key climate response of CMIP6 DECK, historical, and scenario simulations, Geoscientific Model Development, 13, 6165–6200, https://doi.org/10.5194/gmd-13-6165-2020, 2020.

Sellar, A. A., Jones, C. G., Mulcahy, J. P., Tang, Y., Yool, A., Wiltshire, A., O'Connor, F. M., Stringer, M., Hill, R., Palmieri, J., Woodward, S., de Mora, L., Kuhlbrodt, T., Rumbold, S. T., Kelley, D. I., Ellis, R., Johnson, C. E., Walton, J., Abraham, N. L., Andrews, M. B., Andrews, T., Archibald, A. T., Berthou, S., Burke, E., Blockley, E., Carslaw, K., Dalvi, M., Edwards, J., Folberth, G. A., Gedney, N., Griffiths, P. T., Harper, A. B., Hendry, M. A., Hewitt, A. J., Johnson, B., Jones, A., Jones, C. D., Keeble, J., Liddicoat, S., Morgenstern, O., Parker, R. J., Predoi, V., Robertson, E., Siahaan, A., Smith, R. S., Swaminathan, R., Woodhouse, M. T., Zeng, G., and Zerroukat, M.: UKESM1: Description and Evaluation of the U.K. Earth System Model, Journal of Advances in Modeling Earth Systems, 11, 4513–4558, https://doi.org/https://doi.org/10.1029/2019MS001739, 2019.

Steele, M., Morley, R., and Ermold, W.: PHC: A Global Ocean Hydrography with a High-Quality Arctic Ocean, Journal of Climate, 14, 2079 – 2087, https://doi.org/10.1175/1520-0442(2001)014<2079:PAGOHW>2.0.CO;2, 2001.

Swart, N. C., Cole, J. N. S., Kharin, V. V., Lazare, M., Scinocca, J. F., Gillett, N. P., Anstey, J., Arora, V., Christian, J. R., Hanna, S., Jiao, Y., Lee, W. G., Majaess, F., Saenko, O. A., Seiler, C., Seinen, C., Shao, A., Sigmond, M., Solheim, L., von Salzen, K., Yang, D., and Winter, B.: The Canadian Earth System Model version 5 (CanESM5.0.3), Geoscientific Model Development, 12, 4823–4873, https://doi.org/10.5194/gmd-12-4823-2019, 2019.

Séférian, R., Nabat, P., Michou, M., Saint-Martin, D., Voldoire, A., Colin, J., Decharme, B., Delire, C., Berthet, S., Chevallier, M., Sénési, S., Franchisteguy, L., Vial, J., Mallet, M., Joetzjer, E., Geoffroy, O., Guérémy, J.-F., Moine, M.-P., Msadek, R., Ribes, A., Rocher, M., Roehrig, R., Salas-y Mélia, D., Sanchez, E., Terray, L., Valcke, S., Waldman, R., Aumont, O., Bopp, L., Deshayes, J., Éthé, C., and

Madec, G.: Evaluation of CNRM Earth System Model, CNRM-ESM2-1: Role of Earth System Processes in Present-Day and Future Climate, Journal of Advances in Modeling Earth Systems, 11, 4182–4227, https://doi.org/https://doi.org/10.1029/2019MS001791, 2019.

Yukimoto, S., KAWAI, H., KOSHIRO, T., OSHIMA, N., YOSHIDA, K., URAKAWA, S., TSUJINO, H., DEUSHI, M., TANAKA, T., HOSAKA, M., YABU, S., YOSHIMURA, H., SHINDO, E., MIZUTA, R., OBATA, A., ADACHI, Y., and ISHII, M.: The Meteorological Research Institute Earth System Model Version 2.0, MRI-ESM2.0: Description and Basic Evaluation of the Physical Component, Journal of the Meteorological Society of Japan. Ser. II, 97, 931–965, https://doi.org/10.2151/jmsj.2019-051, 2019.